Peng-Xiao Nie, Yi-Ping Wang, Ying Yang*, Guo-Liang Yuan, Wei Li and Xue-Ting Ren

Epitaxial Growth and Multiferroic Properties of (001)-Oriented $BiFeO_3$-$YMnO_3$ Films

Abstract: In this paper, high-quality multiferroic (1-x) $BiFeO_3$-$x$$YMnO_3$ ($x = 0.05$, 0.10, 0.15) thin films were successfully epitaxially grown on (001)$SrTiO_3$ substrates with $La_{0.67}Sr_{0.33}MnO_3$ buffered layers by pulsed laser deposition (PLD). X-ray diffraction shows the thin films are all single-phase perovskite with preferential orientation along the (001) direction. The (002) diffraction angles of thin films (from 0 to 0.15) shift to right, indicating the decrease of lattice parameters. All $YMnO_3$-doped thin films exhibit strong upward self-poling via piezoelectric force microscope (PFM) measurement. Saturated ferroelectric hysteresis loops of thin films cannot be obtained even at the frequency of 50 kHz because of large leakage currents. It is noted that BFO-YMO thin films exhibit ferroelectricity considering the PFM and ferroelectric test. The magnetization measurements show that all $BiFeO_3$-based films exhibit weak ferromagnetic behaviors with saturated magnetization at room temperature. The enhancement of magnetization was observed because of YMO doping, with the maximum saturation magnetization (M_s) of 17.07 emu/cm^3 in $x = 0.10$ thin film.

Keywords: multiferroic, $BiFeO_3$, epitaxial growth, ferromagnetism

DOI 10.1515/ehs-2014-0054

***Corresponding author: Ying Yang,** State Key Laboratory of Mechanics and Control of Mechanical Structures, Nanjing University of Aeronautics and Astronautics, Nanjing 210016, China, E-mail: yingyang@nuaa.edu.cn

Peng-Xiao Nie, College of Materials Science and Technology, Nanjing University of Aeronautics and Astronautics, Nanjing 210016, China; State Key Laboratory of Mechanics and Control of Mechanical Structures, Nanjing University of Aeronautics and Astronautics, Nanjing 210016, China, E-mail: pengxiaonie@nuaa.edu.cn

Yi-Ping Wang, State Key Laboratory of Mechanics and Control of Mechanical Structures, Nanjing University of Aeronautics and Astronautics, Nanjing 210016, China

Guo-Liang Yuan, Department of Materials Science and Engineering, Nanjing University of Science and Technology, Nanjing 210094, China

Wei Li, Xue-Ting Ren, College of Materials Science and Technology, Nanjing University of Aeronautics and Astronautics, Nanjing 210016, China; State Key Laboratory of Mechanics and Control of Mechanical Structures, Nanjing University of Aeronautics and Astronautics, Nanjing 210016, China

Introduction

Multiferroics, a material with intriguing coexistence of electric and magnetic orderings in the same phase, has been widely studied for potential applications in information storage and sensors. Bismuth Ferrite ($BiFeO_3$, BFO) with rhombohedral distorted perovskite structure (ABO_3) is one of well-known multiferroics because of its ferroelectricity (T_C~1103 K) and above-room-temperature antiferromagnetism (T_N~643 K) (Eerenstein, Mathur, and Scott 2006; Wang, Liu, and Ren 2009). However, for BFO ceramics, the measured polarization is small, which is possibly owing to the high leakage. In addition, the spatially modulated spin orderings of Fe^{3+} make it difficult to observe magnetism in bulk BFO at room temperature (Wang, Liu, and Ren 2009). To overcome these obstacles, a large amount of work focuses on preparing high-quality epitaxial BFO films, which may be more promising for practical applications (Prellier, Singh, and Murugavel 2005). With the impact of single crystal substrates strain, epitaxial BFO films grown successfully behave better in polarization switching, piezoelectric response, ferroelectric and magnetic properties (Wang et al. 2003; You et al. 2009; Yun et al. 2004).

During recent decades, many researchers have paid more attention in cations doping to enhance the ferroelectric, piezoelectric and magnetic properties of BFO ceramics and thin films. Yan et al. fabricated lanthanide rare-earth ions (Ln) (e.g. Ce, Eu and Yb) doped BFO thin films, and studied the changes which the Ln-ions would bring to ferroelectricity and piezoelectric responses (Yan, Lai, and Lu 2012). Substitution Mn at Fe-site would significantly change helical spin structure of pure BFO and enhance magnetic properties (Zhao et al. 2013; Sosnowska et al. 2002). Moreover, Silva's group observed the effects of Y and Mn co-doping in BFO ceramics on structural, electrical and magnetic properties (Silva et al. 2012). Hexagonal manganite $YMnO_3$ (YMO) is another type of multiferroic with a ferroelectric Curie temperature $T_C = 950$ K and an antiferromagnetic Neel temperature $T_N = 77$ K (Choi et al. 2010; Vanaken et al. 2004). Considering the effects other multiferroic materials incorporated $BiFeO_3$ may bring, more reports deserve to be carried out, especially on its structural, piezoelectric response, ferroelectric and magnetic

properties. Therefore, our research substituted Y into Bi-site and Mn into Fe-site and systematically observed the role of YMO substitution in BFO-YMO solid solution thin films. In this study, (1-x)BFO-xYMO($x = 0.05$, 0.10, 0.15) solid solution epitaxial thin films were successfully prepared on (001)-oriented $SrTiO_3$ (STO) substrates by pulsed laser deposition (PLD), which could be observed from X-ray diffraction (XRD) patterns and Atomic force microscopy (AFM) images. The strong piezoelectric response, ferroelectric and enhanced magnetic properties of BFO-YMO thin films were investigated.

Experiments

(1-x)$BiFeO_3$-$x$$YMnO_3$($x = 0$~0.15) ceramic targets were synthesized by conventional solid state method with 10 wt.% excess Bi. The excess Bi in ceramics would compensate for the Bi volatilization during thin film preparation. $BiFeO_3$-$YMnO_3$ (BFO-YMO) films (~100 nm) were deposited on (001) oriented $SrTiO_3$ (STO) substrates with $La_{0.67}Sr_{0.33}MnO_3$ (LSMO) buffered layers by pulsed laser deposition (PLD). The frequency of KrF laser ($\lambda = 248$ nm) was 2 Hz with an energy density of 5 J/cm^2 on the target surface, and the deposition temperature was 650°C with 13 Pa oxygen pressure. After deposition, the films were annealed at the same condition for 20 min and cooled to room temperature at the rate of 5°C/min.

The phase and crystal structure of films was characterized with X-ray diffraction (XRD) using Cu $K\alpha$ radiation from a Bruker D8 Advance diffractometer. Atomic force microscope (AFM) with a piezoelectric force microscope (PFM) mode (Bruker multimode 8) was employed to measure surface morphologies and piezoelectric responses of the thin films. Conductive Pt-Ti-coated silicon cantilevers were used for PFM imaging and polarization switching studies. In order to test macroscopic ferroelectric behavior, a ferroelectric capacitor was made by depositing Pt top electrodes upon the as-grown BFO-YMO thin film through a shadow mask. The polarization-electric field (P-E) hysteresis loops of ferroelectric capacitors were measured using a ferroelectric tester (Radiant Technologies, USA). Magnetic measurements at room temperature were performed using Vibrating Sample Magnetometer (VSM) from a Physical Property Measurement System (PPMS, Quantum Design). The size of sample was limited to 3 mm × 3 mm, and the applied magnetic field ranging from −8 kOe to 8 kOe was parallel to the surface of thin film.

Results and Discussions

(1-x)BFO-xYMO ($x = 0$~0.15) solid solution thin films grown in a rhombohedral structure along with (100)-oriented STO single crystal substrates were shown in Figure 1. Only diffraction peaks from (001) and (002) planes of substrates and (1-x)BFO-xYMO thin films are observed without impurity or other phases, indicating the epitaxial growth of BFO-YMO thin films upon (001) STO were successfully made. The (002) diffraction angles of (1-x)BFO-xYMO ($x =$ 0, 0.05, 0.10, 0.15) thin films are 44.46°, 44.88°, 45.32°, and 45.75°, respectively, suggesting the decrease of lattice parameters. This is due to the ionic radius of Y and Mn are 0.9 Å and 0.46 Å, while Bi and Fe are 1.03 Å and 0.645 Å. Therefore, with the addition of Y and Mn substitutions at A-site and B-site cations of BFO, the lattice parameters gradually decrease and the lattice distortions become larger. Moreover, the in-plane crystal lattice parameters are $a = b \approx 0.391$ nm for STO, $a = b \approx 0.387$ nm for LSMO and $a \approx b \approx 0.396$ nm for pure BFO in theory (Chen et al. 2013), thus there are compressive strain in BFO/LSMO/STO structure thin films. Moreover, the BFO-YMO thin films' compressive strain gradually relaxes originated from the decrease of lattice parameters owing to the addition of YMO (Luo et al. 2013).

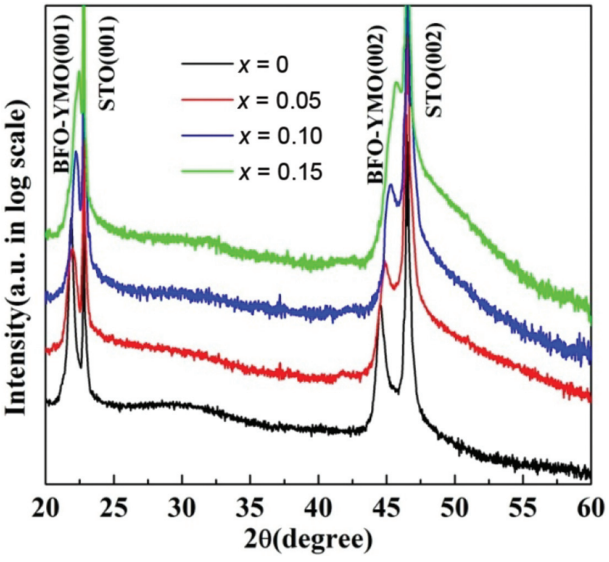

Figure 1: Room temperature X-ray diffraction spectra of the (1-x)BFO-xYMO thin films in log scale.

The topographies, PFM out-of-plane (OP) phases, and OP amplitudes of (1-x)BFO-xYMO ($x = 0.05$, 0.10, 0.15) samples are shown in Figure 2. The surface morphologies

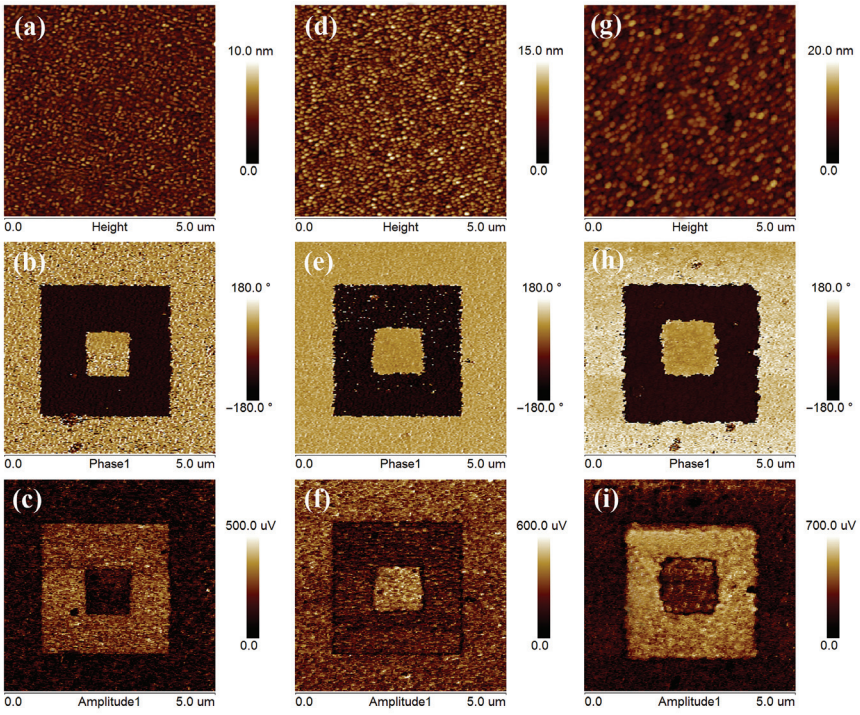

Figure 2: The morphologies, OP phases, and OP amplitudes of (a)–(c) 0.95BFO–0.05YMO, (d)–(f) 0.90BFO–0.10YMO, and (g)–(i) 0.85BFO–0.15YMO thin films.

of $x = 0.05$, 0.10 and 0.15 (Figure 2(a), (d), (g)) thin films with a scanning area of $5 \times 5\ \mu m^2$ are all flat and smooth without obvious cracks or discontinuities. The roughness of these samples is ~10 m, ~15 nm and ~20 nm, respectively, which all suggests island growth. It is clearly that island growth generates rough surface compared with layer-by-layer growth, which would leads to atomic smooth surface (Yuan et al. 2013). Moreover, we use Nanoscope Analysis software to calculate average grain size, root-mean-square (RMS) surface roughness (R_q) and average surface roughness (R_a) of thin films. The average grain size of (1-x)BFO-xYMO ($x = 0.05$, 0.10, 0.15) films were calculated to be 160, 190 and 230 nm, respectively. And the R_q of $x = 0.05$, 0.10, 0.15 films are 2.46, 3.19 and 3.36 nm, while the R_a of which are 1.81, 2.35 and 2.39 nm. These slightly change of grain sizes may be due to the increase of lattice distortion. It is known that the morphological characteristic of samples highly depends on the growth conditions, including deposition temperature and oxygen partial pressure. Thus with the above mentioned growth condition, high-quality epitaxial thin films can be prepared.

Figure 2 (b), (e), (h) shows OP PFM phases of corresponding areas of (1-x)BFO-xYMO ($x = 0.05$, 0.10, 0.15) obtained after the $3 \times 3\ \mu m^2$ region was polarized with −8V sample bias and the central $1 \times 1\ \mu m^2$ region was polarized with 8V sample bias upon LSMO bottom electrode, respectively. As shown in Figure 2(e), the phase degree of the as-grown film outside the $3 \times 3\ \mu m^2$ region with no polarized sample bias shows the same yellow color as that of the central 8V polarized region, suggesting both of their polarizations are upward. It is noted that $x = 0.10$ thin film exhibits a strong upward spontaneous polarization. Similar polarization switching phenomenon can also be observed in $x = 0.05$ and $x = 0.15$ thin films. Black dots embedded in yellow matrix, as shown in Figure 2(h), suggests a weak self-poling. Figure 2(c), (f) and (i) show the OP PFM amplitudes of (1-x)BFO-xYMO ($x = 0.05$, 0.10, 0.15) samples with corresponding areas. The amplitude phenomenon of 8V polarized, −8V polarized and no polarized regions shows obvious differences, which also proves films' polarization switching and piezoelectric response.

Polarization versus electric field (P-E) hysteresis loops of (1-x)BFO-xYMO ($x = 0.05$, 0.10, 0.15) with a frequency of 50 kHz are shown in Figure 3. All the BFO-YMO films cannot reach fully saturations due to the semiconducting nature which the large leakage currents became

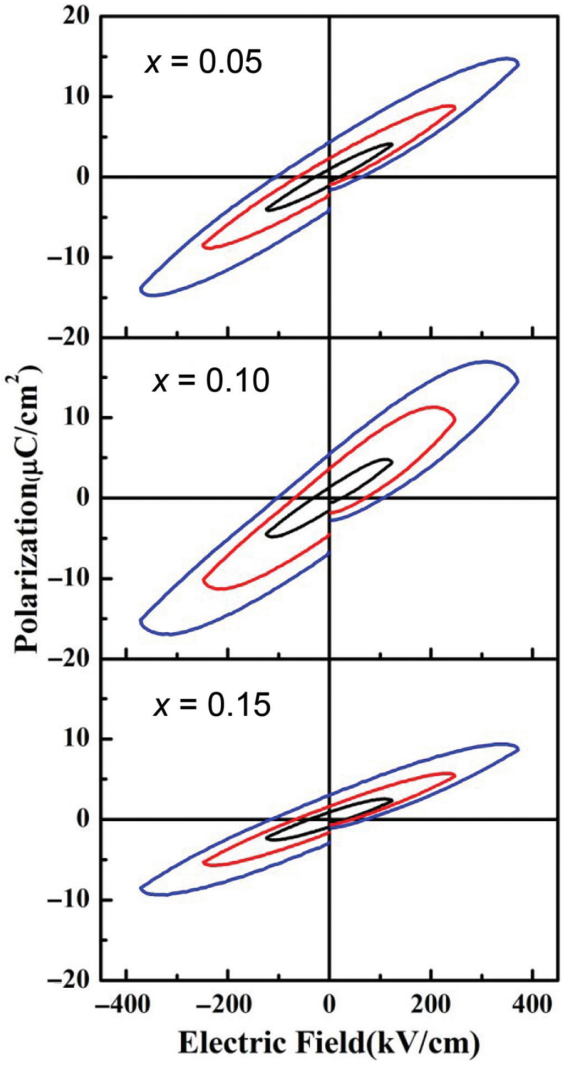

Figure 3: Room temperature electric hysteresis loops of (1-*x*)BFO-*x*YMO thin films at 50 kHz.

significant. In general, it is not easy to measure the stable P-E loops in the high electric field because of the poor breakdown properties (Kawae et al. 2009). However, combined with previous spontaneous polarization measured by PFM in Figure 2, the BFO-YMO thin films indeed exhibit ferroelectric properties. The coupling with low resistance made it difficult to obtain saturated ferroelectric hysteresis loops in BFO-based thin films, although some improved P-E loops have been reported (You et al. 2009; Das et al. 2006). Wang et al. reported that the ferroelectricity of the BFO thin films attributed from the displacement of Bi^{3+} with respect to the FeO_6 cages along the (111) plane (Wang et al. 2003). The remnant polarization value $2P_r$ is 11.5 μC/cm^2 for the 0.90BFO–0.10YMO film with an obvious leakage current, which is much smaller than some reported studies. The poor ferroelectric properties of BFO-YMO indicate that the substitution of Y cations for $Bi^{3\pm}$ cannot reduce the leakage current effectively.

The magnetic hysteresis (*M-H*) curves measured at 300 K with a maximum magnetic field of 8 kOe applied along the in-plane direction are shown in Figure 4. All the epitaxial (1-*x*)BFO-*x*YMO ($x = 0$, 0.05, 0.10, 0.15) films can be found to exhibit a weak ferromagnetic behavior. It is observed that the magnetization increased rapidly with the increase in magnetic field (H) up to 4 kOe and thereafter tends to saturate for all samples, indicating the ferroelectric behaviors. As reported that the saturation magnetization (M_s) of the epitaxially grown films correlates well with the magnitude of the misfit strain (Ryu et al. 2009), the ~100 nm (001)-oriented pure BFO film shows a M_s of 5.26 emu/cm^3 in Figure 4. Several factors such as the interface strain and enhanced anisotropy of BFO thin films would significantly induce the destruction of a spatially modulated cycloidal spin structure in bulk BFO, resulting in release of a latent antiferromagnetic component locked within the cycloid (Bai et al. 2005). One prominent feature of Figure 4 is that the magnetization obviously enhanced with the addition of YMO substitution. As shown in Figure 4, the M_s of (1-*x*)BFO-*x*YMO ($x = 0.05$, 0.10, 0.15) films are 13.66, 17.07 and 11.25 emu/cm^3, respectively. Combined with relative literatures (Sosnowska et al. 2002) and previous studies, it seems that incorporated Mn^{3+} would mainly be responsible for magnetic improvement of BFO-YMO thin film system, including weak canting of spin moments because of coupling with polarization and the distortion in the spin

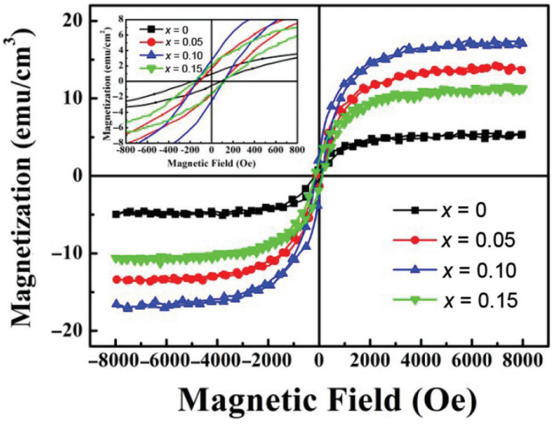

Figure 4: Magnetic hysteresis loops of (1-*x*)BFO-*x*YMO (*x* from 0 to 0.15) thin films at 300 K.

cycloid structure when Mn ions with a different valence and size are substituted randomly at the Fe site (Catalan and Scott 2009). However, the small decrease in the magnetic behavior of 0.85BFO–0.15YMO thin film was observed, owing to cation-anion-cation exchange interaction at an octahedral site (Gupta et al. 2012). The double ion interaction in Fe-O-Mn would be responsible for magnetization effect while Fe-O-Fe and Mn-O-Mn interaction in the same lattice cancel the magnetization. Hence, with the addition of Mn concentration (up to 10%), magnetization enhanced as a result of double ion interaction with canting distortion effect. When the $x > 0.10$, the Mn–O–Mn interaction increased with the increase of Mn concentration, leading to slight decrease of magnetization. Magnetic hysteresis loops shown in Figure 4 revealed a quite low coercivity, which would be a special feature of soft magnetic materials for a wide range of potential applications.

Conclusion

(1-x)$BiFeO_3$-$xYMnO_3$($x = 0.05$, 0.10, 0.15) solid solution epitaxial thin films were successfully grown upon (001) $SrTiO_3$ substrates with $La_{0.67}Sr_{0.33}MnO_3$ buffered layers. The lattice parameters of films decrease and lattice distortions increase with the addition of YMO concentration. Strong spontaneous polarizations were observed by PFM images and all BFO-YMO thin films exhibit ferroelectric properties. Moreover, doping YMO greatly enhances the magnetization of the thin films, which observed by VSM. 0.90BFO-0.10YMO thin films exhibit an optimal magnetic property of $M_s = 17.07$ emu/cm^3.

Funding: The work was financially supported by the National Natural Science Foundation of China (No. 11274174), the National Key Project for Basic Research of China (2012CB619406), the 111 project (Grant no. B12021), the Foundation of Graduate Innovation Center in NUAA (No. kfjj201469) and the Fundamental Research Funds for the Central Universities.

References

Bai, F., J. Wang, M. Wuttig, et al. 2005. "Destruction of Spin Cycloid in (111) c-Oriented $BiFeO_3$ Thin Films by Epitaxial Constraint: Enhanced Polarization and Release of Latent Magnetization." *Applied Physics Letters* 86 (3): 032511–032511–3.

Catalan, G., and J. F. Scott. 2009. "Physics and Applications of Bismuth Ferrite." *Advanced Materials* 21 (24): 2463–85.

Chen, A., Z. Bi, Q. Jia, et al. 2013. "Microstructure, Vertical Strain Control and Tunable Functionalities in Self-Assembled, Vertically Aligned Nanocomposite Thin Films." *Acta Materialia* 61 (8): 2783–92.

Choi, T., Y. Horibe, H. T. Yi, et al. 2010. "Insulating Interlocked Ferroelectric and Structural Antiphase Domain Walls in Multiferroic $YMnO_3$." *Nature Materials* 9 (3): 253–58.

Das, R. R., D. M. Kim, S. H. Baek, et al. 2006. "Synthesis and Ferroelectric Properties of Epitaxial $BiFeO_3$ Thin Films Grown by Sputtering." *Applied Physics Letters* 88 (24): 242904.

Eerenstein, W., N. D. Mathur, and J. F. Scott. 2006. "Multiferroic and Magnetoelectric Materials." *Nature* 442 (7104): 759–65.

Gupta, S., A. Sharma, M. Tomar, et al. 2012. "Piezoresponse Force Microscopy and Vibrating Sample Magnetometer Study of Single Phased Mn Induced Multiferroic $BiFeO_3$ Thin Film." *Journal of Applied Physics* 111 (6): 064110.

Kawae, T., Y. Terauchi, H. Tsuda, et al. 2009. "Improved Leakage and Ferroelectric Properties of Mn and Ti Codoped $BiFeO_3$ Thin Films." *Applied Physics Letters* 94 (11): 112904–112904–3.

Luo, Y., X. Li, L. Chang, et al. 2013. "Upward Ferroelectric Self-Poling in (001) Oriented $PbZr0._2Ti_{0.8}O_3$ Epitaxial Films with Compressive Strain." *AIP Advances* 3 (12): 122101.

Prellier, W., M. P. Singh, and P. Murugavel. 2005. "The Single-Phase Multiferroic Oxides: From Bulk to Thin Film." *Journal of Physics: Condensed Matter* 17 (30): R803.

Ryu, S., J. Y. Kim, Y. H. Shin, et al. 2009. "Enhanced Magnetization and Modulated Orbital Hybridization in Epitaxially Constrained BiFeO3 Thin Films with Rhombohedral Symmetry." *Chemistry of Materials* 21 (21): 5050–57.

Silva, J., A. Reye, R. Castañeda, et al. 2012. "Structure and Electromagnetic Properties of $Bi_{1-x}Y_xFe_{0.95}Mn_{0.05}O_3$ ($x = 0.05$, 0.075 and 0.10)." *Ferroelectrics* 426 (1): 103–11.

Sosnowska, I., W. Schäfer, W. Kockelmann, et al. 2002. "Crystal Structure and Spiral Magnetic Ordering of $BiFeO_3$ Doped with Manganese." *Applied Physics A* 74 (1): s1040–s1042.

Vanaken, B. B., T. T. Palstra, A. Filippetti, et al. 2004. "The Origin of Ferroelectricity in Magnetoelectric $YMnO_3$." *Nature Materials* 3 (3): 164–70.

Wang, K. F., J. M. Liu, and Z. F. Ren. 2009. "Multiferroicity: The Coupling Between Magnetic and Polarization Orders." *Advances in Physics* 58 (4): 321–448.

Wang, J., J. B. Neaton, H. Zheng, et al. 2003. "Epitaxial $BiFeO_3$ Multiferroic Thin Film Heterostructures." *Science* 299 (5613): 1719–22.

Yan, F., M. O. Lai, and L. Lu. 2012. "Domain Structure and Piezoelectric Response in Lanthanide Rare Earth-Substituted Multiferroic $BiFeO_3$ Thin Films." *Journal of Physics D: Applied Physics* 45 (32): 325001.

You, L., N. T. Chua, K. Yao, et al. 2009. "Influence of Oxygen Pressure on the Ferroelectric Properties of Epitaxial $BiFeO_3$ Thin Films by Pulsed Laser Deposition." *Physical Review B* 80 (2): 024105.

Yuan, G., J. Chen, H. Xia, et al. 2013. "Ferroelectric Domain Evolution with Temperature in $BaTiO_3$ Film on (001) $SrTiO_3$ Substrate." *Applied Physics Letters* 103 (6): 062903.

Yun, K. Y., M. Noda, M. Okuyama, et al. 2004. "Structural and Multiferroic Properties of $BiFeO_3$ Thin Films at Room Temperature." *Journal of Applied Physics* 96 (6): 3399–403.

Zhao, X. Q., W. Wang, C. Zheng, et al. 2013. "Ferroelectric, Electrical, and Magnetic Properties of $BiFe_{0.95}Mn_{0.05}O_3$ Thin Films Epitaxially Grown on Conductive Nb: $SrTiO_3$ and $La_{0.7}Sr_{0.3}MnO_3$-Buffered Nb: $SrTiO_3$ Substrates." *Journal of Materials Science: Materials in Electronics* 24 (5): 1677–84.